STM JOURNALS

Journal of
Polymer & Composites

ISSN: 2321-2810 (Online)
ISSN: 2321-8525 (Print)
Volume 13, Issue 6, 2025
DOI (Journal): 10.37591/JoPC

https://journals.stmjournals.com/jopc/

Research JoPC

Influence of Carbonyl Iron Particle Loading on the Dimensional and Rheological Properties of 4D-Printed TPU-Based Magnetorheological Elastomers

Ahmad Fitri Sukarman[1], Norasyidah Mohd Noh[2], Nurulhuda Khalid[3], Saiful Amri Mazlan[4,*], Mohd Aidy Faizal Johari[5], Muhammad Farhan Mohamad Fitri[6], Shahir Mohd Yusuf[7], Nur Azmah Nordin[8], Abdul Yasser Abd Fatah[9]

Abstract

The advancement of 4D printing technologies has created new opportunities for fabricating smart materials with tunable properties, including magnetorheological elastomers (MREs). This study investigates the fabrication and characterization of thermoplastic polyurethane (TPU)-based MREs with varying carbonyl iron particle (CIP) loadings (10–50 wt.%) using the fused filament fabrication (FFF) method. MRE filaments were produced through a solvent-assisted mixing and extrusion process, ensuring consistent diameters within 1.75 ± 0.10 mm. Test specimens were printed under fixed processing parameters to assess printability, dimensional fidelity, mechanical hardness, and rheological behaviour. Results showed that all FFF-printed MREs achieved high dimensional accuracy, with deviations below 5.5%, and exhibited a progressive increase in Shore A hardness and off-state storage modulus (G') with higher CIP content. Under an applied magnetic field, all samples displayed the magnetorheological effect, with stiffness enhancement proportional to CIP loading. Comparative analysis with previously reported fused granulate fabrication (FGF)-printed MREs revealed that FFF yields higher baseline stiffness but a comparatively lower MR effect, attributed to anisotropic particle alignment during filament extrusion. These findings highlight the trade-offs between dimensional precision, inherent stiffness, and field responsiveness in additively manufactured MREs, providing valuable insights for their application in adaptive structures, tunable damping systems, and soft robotic actuators.

***Author for Correspondence**
Saiful Amri Mazlan
E-mail: amri.kl@utm.my

[1]Student, Department of Engineering Materials and Structures (eMast) iKohza, Malaysia-Japan International Institute of Technology (MJIIT), Universiti Teknologi Malaysia (UTM), Kuala Lumpur, Malaysia.
[2,3]Lecturer, Department of Mechanical Engineering, Politeknik Banting Selangor, Banting, Malaysia.
[4]Professor, Department of Engineering Materials and Structures (eMast) iKohza, Malaysia-Japan International Institute of Technology (MJIIT), Universiti Teknologi Malaysia (UTM), Kuala Lumpur, Malaysia.
[5]Post Doctoral, Department of Engineering Materials and Structures (eMast) iKohza, Malaysia-Japan International Institute of Technology (MJIIT), Universiti Teknologi Malaysia (UTM), Kuala Lumpur, Malaysia.
[6]Student, Department of Engineering Materials and Structures (eMast) iKohza, Malaysia-Japan International Institute of Technology (MJIIT), Universiti Teknologi Malaysia (UTM), Kuala Lumpur, Malaysia.
[7,8]Senior Lecturer, Department of Engineering Materials and Structures (eMast) iKohza, Malaysia-Japan International Institute of Technology (MJIIT), Universiti Teknologi Malaysia (UTM), Kuala Lumpur, Malaysia.
[9]Senior Lecturer, Department of Smart Engineering and Advanced Technology, Faculty of Artificial Intelligence, Universiti Teknologi Malaysia (UTM), Kuala Lumpur, Malaysia.

Received Date: August 26, 2025
Accepted Date: September 05, 2025
Published Date: October 08, 2025

Citation: Ahmad Fitri Sukarman, Norasyidah Mohd Noh, Nurulhuda Khalid, Saiful Amri Mazlan, Mohd Aidy Faizal Johari, Muhammad Farhan Mohamad Fitri, Shahir Mohd Yusuf, Nur Azmah Nordin, Abdul Yasser Abd Fatah. Influence of Carbonyl Iron Particle Loading on the Dimensional and Rheological Properties of 4D-Printed TPU-Based Magnetorheological Elastomers. Journal of Polymer & Composites. 2025; 13(6): 127–138p.

Keywords: 4D printing, 3D printing, fused filament fabrication, fused granulate fabrication, magnetorheological elastomer

INTRODUCTION

Additive Manufacturing (AM), commonly referred to as 3D printing, has transformed the production of complex, customized parts by enabling layer-by-layer fabrication with minimal

waste, reduced lead times, and a high degree of design freedom. Unlike subtractive manufacturing, AM builds components directly from digital models, thereby streamlining prototyping and facilitating low-volume production runs without the need for extensive tooling. This capability extends to a wide range of materials including polymers, metals, ceramics, and composites, supporting applications in diverse sectors such as aerospace, biomedical engineering, and automotive manufacturing [1, 2]. The emergence of 4D printing has further expanded the potential of AM by introducing the concept of time-dependent functionality, where printed structures are fabricated from stimuli-responsive materials capable of changing shape, mechanical properties, or functional behaviour over time in response to external triggers such as temperature, light, moisture, pH, or magnetic fields [3]. By integrating material science with AM process control, 4D printing offers unprecedented opportunities to create adaptive, multifunctional components that surpass the static limitations of conventional manufacturing.

Among the most promising 4D printable smart materials are magnetorheological elastomers (MREs), which are composites consisting of micron-sized magnetic particles embedded within an elastomeric matrix. When subjected to an external magnetic field, the magnetic particles align into chain-like structures, leading to rapid and reversible changes in the composite's mechanical properties, particularly stiffness and damping capacity. This unique magneto-responsive behaviour makes MREs attractive for vibration isolation systems, adaptive stiffness control devices, soft robotics, and tunable damping mechanisms [4, 5]. However, traditional MRE fabrication methods, such as moulding and casting, often involve multi-step processes with high tooling costs, long cycle times, and restricted design flexibility. Furthermore, these methods are ill-suited for producing geometrically intricate or customized components, and scaling production while maintaining consistent particle distribution remains challenging [6]. These limitations have driven increasing interest in AM-based MRE manufacturing, which combines the functional versatility of MREs with the geometric precision, scalability, and rapid prototyping capabilities of additive manufacturing technologies.

Early research efforts in AM-based MRE fabrication largely focused on Direct Ink Writing (DIW), where a viscous MRE paste or slurry is extruded through a nozzle to form the desired geometry [7, 8]. While DIW allows for high magnetic particle loadings and custom formulations, its reliance on highly viscous feedstock results in slow printing speeds, high extrusion pressures, and an increased risk of nozzle clogging. Furthermore, DIW typically delivers lower geometric precision and surface finish due to inconsistencies in extrusion flow and limited capability for fine feature resolution. Post-processing steps, such as curing or solvent evaporation, are often necessary, which complicates the manufacturing process. To address some of these issues, Fused Granulate Fabrication (FGF) has been explored as an alternative. In this method, polymer granules mixed with magnetic particles are directly fed into a heated extruder [9, 10]. FGF offers higher deposition rates, broader material compatibility including the use of recycled or modified thermoplastics, and eliminates the need for filament pre-production. However, these advantages come at the expense of dimensional accuracy and surface quality, since the larger nozzle diameters and higher layer heights typically used in FGF produce coarser resolution and more visible layer lines. Rapid granule extrusion can also introduce incomplete interlayer fusion and internal voids, which compromise mechanical integrity. Additionally, particle dispersion can be uneven, especially at higher loadings, potentially reducing the uniformity of the magnetorheological effect. On another method, Fused Filament Fabrication (FFF) offers a promising route to overcome many of these limitations. By using pre-extruded fine-diameter filaments, typically 1.75 or 2.85 mm, FFF enables higher resolution, tighter dimensional tolerances, and improved surface finish compared to FGF. These qualities are particularly important when fabricating functional prototypes or components with intricate geometries where precision and repeatability are critical [11]. The filament-based approach also facilitates more controlled material feeding, potentially improving particle dispersion and reducing void formation. Despite these advantages, there is limited research on the fabrication of MREs via FFF, and even fewer studies that directly compare the mechanical and rheological performance of FFF-printed MREs with their FGF-printed counterparts. In particular, the role of carbonyl iron particle (CIP) loading in influencing FFF-printed MREs' printability, dimensional fidelity, and magneto-responsive performance remains poorly understood, representing a clear research gap that this study aims to address.

Therefore, the present study focuses on the fabrication of thermoplastic polyurethane (TPU)-based magnetorheological elastomer (MRE) filaments with varying carbonyl iron particle (CIP) loadings ranging from 10 to 50 wt.% for 4D printing using the Fused Filament Fabrication (FFF) method. The investigation examines the feasibility of producing defect-free MRE filaments and printed parts with consistent filament diameter, high dimensional fidelity, and surface quality suitable for functional applications, while also determining how CIP concentration influences the mechanical hardness and geometrical accuracy of the printed structures. Furthermore, the rheological response of the MREs is characterized under varying magnetic field strengths to assess their magneto-mechanical performance and suitability for adaptive and tunable devices. A comparative analysis with previously reported Fused Granulate Fabrication (FGF)-printed MREs is conducted to identify the advantages and limitations of the filament-based approach, with particular attention to the trade-offs between baseline mechanical stiffness and magnetorheological effect. By addressing the current knowledge gap on the effect of particle loading in filament-based MRE printing, the findings from this study are expected to provide practical guidelines for optimizing both material formulation and printing parameters, ultimately supporting the design and manufacturing of next-generation 4D printable MREs for applications in adaptive structures, tunable damping systems, vibration isolation devices, and soft robotic actuators.

METHODOLOGY

This section outlines the procedures used to fabricate and characterize TPU-based MREs with varying CIP loadings via the FFF process. The methodology covers the preparation of composite filaments through a solvent-assisted mixing and extrusion process, the printing of test specimens under controlled parameters, and the measurement techniques used to evaluate dimensional accuracy, mechanical hardness, and rheological behaviour. Each stage was designed to ensure consistency across samples so that the influence of CIP concentration on printability, stiffness, and magneto-responsive performance could be reliably assessed and compared with previously reported FGF results.

MRE Sample Preparation Process

The MRE samples in this study were prepared by incorporating CIPs into a TPU matrix, followed by filament extrusion and 4D printing via the FFF process. Pellet Flex-based TPU pellets (Smart Material 3D, Alcalá la Real, Spain) were selected as the matrix material due to their high flexibility and durability, with a Shore hardness of 90A and pellet diameters of 2–4 mm. As the magnetic filler, spherical OM-grade CIPs (BASF, Ludwigshafen, Germany) with diameters of 3–5 μm were used, offering high magnetic saturation, high permeability, and low remnant magnetization [12]. Tetrahydrofuran (THF) (R&M Chemical, Kuala Lumpur, Malaysia) was used as the solvent to dissolve TPU pellets during composite formulation.

Prior to mixing, TPU pellets were dried in a Sunlu S1 Plus dryer box (Zhuhai, China) at 50 °C for 2 hours to remove residual moisture, thereby preventing bubble formation during filament extrusion. The dried TPU was then dissolved in THF at 50 °C under continuous mechanical stirring at 250 rpm in a fume hood [13]. CIPs were gradually introduced into the TPU solution to achieve target weight fractions of 10, 20, 30, 40, and 50 wt.%, maintaining uniform dispersion by stirring for 1.5 hours at the same temperature and agitation rate. This solvent-assisted mixing method ensured homogenous particle distribution and minimized agglomeration.

The resulting mixtures were cast into Petri dishes and left to dry at ambient conditions for 24 hours to allow complete solvent evaporation. The dried composites were then cut into small granules (<5 mm) to facilitate smooth feeding into the filament extruder. Filament production was carried out using a Noztek Pro single-barrel extruder (Noztek, Shoreham, England) at a controlled extrusion rate of 2.5 m/min. The target filament diameter was 1.75 ± 0.10 mm, matching the specifications for the 3D printer. Diameters were measured at 10 evenly spaced points along the filament to ensure dimensional consistency and compliance with printing requirements. The overall process of fabricating MRE filament is shown in Figure 1.

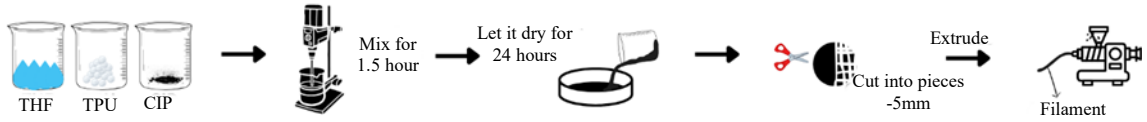

Figure 1. MRE filament preparation process.

Figure 2. Artillery sidewinder X1.

4D Printing via FFF

Fabrication of the test specimens was performed using an Artillery Sidewinder SW-X1 desktop 3D printer (Artillery 3D, Hong Kong) equipped with a standard filament extruder and a 0.4 mm nozzle as shown in Figure 2.

The CAD models, designed in Fusion 360 with a cylindrical geometry of 20 mm diameter and 1 mm thickness, were sliced using UltiMaker Cura 5.7.1 software to generate the G-code. Based on the printer manufacturer's guidelines, the nozzle temperature was set at 210 °C for pure TPU and was maintained at the same setting for all MRE formulations to ensure comparable processing conditions. Printing parameters including layer height, bed temperature, infill density, infill pattern, and printing speed, were kept constant for all samples to isolate the effects of CIP content on printability and performance (Table 1). These parameters were selected following the printer manufacturer's recommendations and prior studies on TPU-based composites, ensuring stable extrusion and comparability across formulations [13]. This controlled approach ensured that any observed differences in dimensional accuracy or mechanical properties could be attributed to the variation in particle loading rather than changes in processing parameters.

Dimensional and Hardness Measurements

Printed specimens were measured using a digital vernier calliper to assess conformity with the CAD model, with deviations expressed as percentages relative to nominal dimensions. All samples maintained dimensional deviations below 5.5%, demonstrating stable printing performance across the different CIP loadings. Shore A hardness measurements were conducted in accordance with ASTM D2240, with five replicates per sample to ensure statistical reliability.

Table 1. 4D printing parameters of MRE.

Parameter	Value
Layer Height	0.2 mm
Nozzle diameter	0.4 mm
Infill density	100%
Infill pattern	Grid
Nozzle temperature	210°C
Bed temperature	60°C
Printing Speed	25 mm/s

Rheological Testing

Rheological behaviour was characterized using a Physica MCR 302 rheometer (Anton Paar, Graz, Austria) equipped with an MRD 170 magnetorheological device, operating in oscillatory shear mode. All measurements were performed at 25 °C under controlled strain and magnetic field conditions. Strain sweep tests were carried out over a strain amplitude range of 0.001–10% at a fixed frequency of 1 Hz to determine the linear viscoelastic (LVE) region for each sample. Magnetic fields corresponding to applied currents of 0, 1, 2, 3, and 4 A (0.003–0.624 T) were applied to evaluate field-dependent stiffness changes. Each test was conducted in triplicate to confirm repeatability. This experimental setup enabled a direct assessment of how particle loading and magnetic field strength influence the magneto-mechanical performance of FFF-printed MREs.

RESULTS AND DISCUSSION

This section presents the experimental findings on the dimensional accuracy, mechanical hardness, and rheological performance of TPU-based MREs fabricated via FFF with varying CIP loadings. The results are interpreted in relation to the research objectives outlined in Section 1 and the fabrication methods described in Section 2, with emphasis on the influence of CIP concentration on both off-state and on-state mechanical behavior. Comparative analysis with previously reported FGF-printed MREs is also included to highlight the differences in dimensional fidelity, baseline stiffness, and magneto-responsive performance between the two additive manufacturing approaches. The discussion integrates microstructural considerations, such as particle dispersion and alignment during filament extrusion, to explain the observed trends and establish their implications for application-specific design of 4D-printed MREs.

Dimensional Characteristics

The printed specimens demonstrated excellent dimensional fidelity across all CIP loadings, highlighting the capability of the FFF process to produce geometrically accurate MRE components. Figure 3 shows the visual comparison between pure TPU and MRE samples, where the incorporation of CIPs results in a distinct darkened appearance proportional to the particle concentration, confirming successful particle integration into the matrix. The grid-line pattern visible on both pure TPU and MRE specimens reflects the programmed infill structure generated during slicing, indicating consistent deposition and adhesion between adjacent filament paths.

The Shore A hardness values in Table 2 reveal a modest but consistent increase with higher CIP loading, from 90.8 A for pure TPU to 92.8 A for MRE50, corresponding to approximately a 2% enhancement in stiffness. This trend is consistent with the reinforcing effect of rigid magnetic particles within the elastomer matrix, as CIPs act as micro-scale load-bearing fillers that restrict polymer chain mobility. At higher particle concentrations, the reduced inter-particle spacing further contributes to rigidity by creating additional resistance points to deformation [14,15]. Although the magnitude of hardness increase is relatively small compared to traditional mould-cast MREs, this can be attributed to the FFF process, where particle alignment along the filament extrusion path may limit isotropic reinforcement.

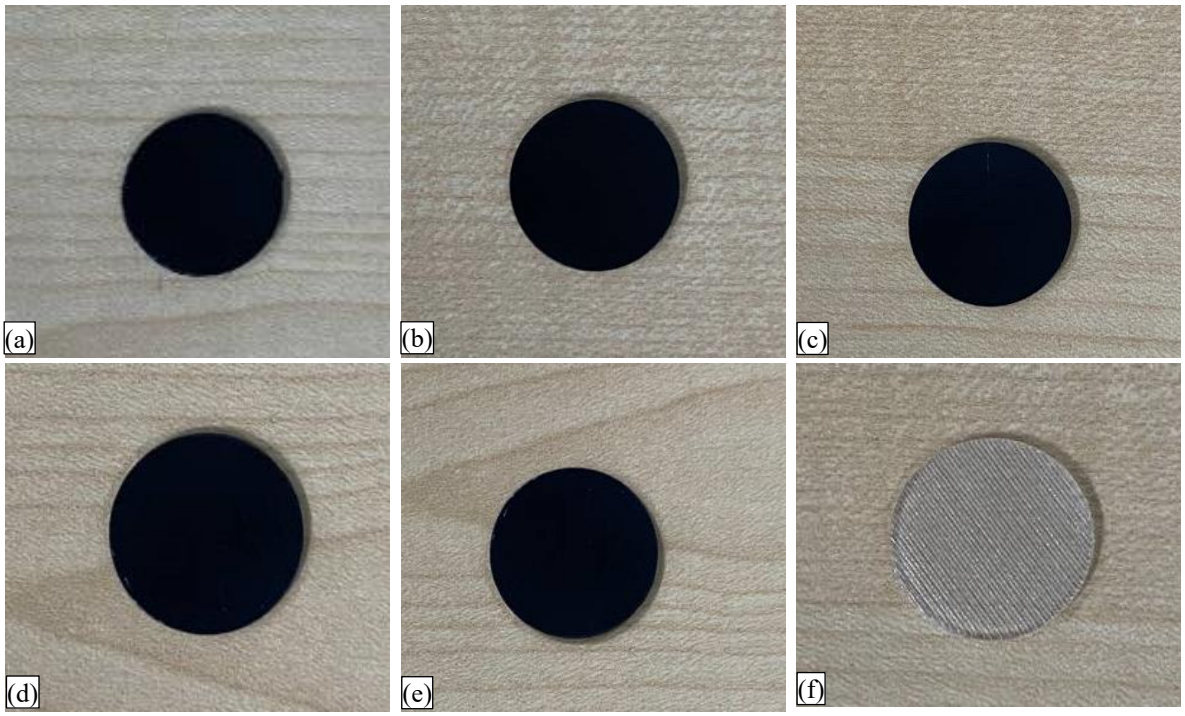

Figure 3. 4D printed MRE samples; (a) MRE10, (b) MRE20, (c) MRE30, (d) MRE40, (e) MRE50, and (f) Pure TPU.

Table 2. Shore A Hardness for Pure TPU and MRE samples.

Sample	Hardness (A)					Average Value (A)
	1	*2*	*3*	*4*	*5*	
Pure TPU	90	91	92	92	89	90.8
MRE10	91	91	91	91	90	90.8
MRE20	92	92	91	91	91	91.4
MRE30	92	91	92	92	91	91.6
MRE40	92	92	91	93	92	92.0
MRE50	93	93	92	93	93	92.8

Table 3. Dimensional characteristics and mean deviations of pure TPU and MRE samples.

Sample	Thickness(mm)			Average Thickness (mm)	Average Deviation (%)	Diameter (mm)			Average Diameter (mm)	Average Deviation (%)
	1	2	3			1	2	3		
Pure TPU	1.11	1.00	1.01	**1.04**	**4.49**	20.0	20.0	20.0	**20.0**	**0.0**
MRE10	1.01	1.10	1.08	**1.06**	**3.46**	20.0	20.0	20.0	**20.0**	**0.0**
MRE20	1.10	1.01	1.06	**1.06**	**2.83**	20.0	20.0	20.0	**20.0**	**0.0**
MRE30	1.17	1.06	1.02	**1.08**	**5.25**	20.0	20.0	20.0	**20.0**	**0.0**
MRE40	1.15	1.13	1.05	**1.11**	**3.60**	20.0	20.0	20.0	**20.0**	**0.0**
MRE50	1.13	1.18	1.14	**1.15**	**2.13**	20.0	20.0	20.0	**20.0**	**0.0**

The dimensional measurements in Table 3 show that the average deviations from the nominal CAD geometry remained below 5.5% for thickness and at 0% for diameter across all compositions, indicating stable layer deposition and minimal thermal distortion during printing. The negligible effect of CIP concentration on dimensional accuracy suggests that the FFF process parameters, particularly the nozzle temperature, bed temperature, and printing speed, were well-optimized for both pure TPU and

composite filaments. This result is significant when compared to FGF, which often suffers from dimensional inaccuracies due to larger nozzle sizes and coarser layer heights [10].

Filament diameter measurements (Table 4) further confirm the high precision of the filament extrusion stage, with all formulations achieving average diameters within the target tolerance of 1.75 ± 0.10 mm. The consistency in filament diameter across all CIP loadings ensured uniform feeding during printing and contributed to the observed dimensional stability of the final parts. This finding aligns with the objectives outlined in the methodology, where achieving a defect-free, dimensionally stable filament was identified as a prerequisite for reliable FFF printing of MREs.

The obtained dimensional characteristics demonstrate that FFF is capable of producing MRE parts with high geometric fidelity and repeatable quality, even at high particle loadings of up to 50 wt.%. These results directly address one of the limitations noted for FGF in the introduction that related to its tendency for lower precision, and confirm that the filament-based approach offers a clear advantage in applications, where tight dimensional tolerances are critical, such as adaptive structures and soft robotic components.

Strain Sweep Analysis

The strain sweep tests were performed to identify the LVE region of the FFF-printed MREs and to assess the influence of CIP loading on their stiffness under both zero-field (off-state) and applied magnetic field (on-state) conditions. The LVE region represents the range of strain over which the material's storage modulus (G′) remains constant, indicating that the internal microstructure is not yet disrupted by deformation. Establishing this region is essential to ensure that subsequent rheological measurements, such as current sweep or frequency sweep, are conducted within the elastic limit, where the measured modulus truly reflects the material's structural integrity.

Figure 4 shows the variation of storage modulus (G′) as a function of shear strain (γ) over a range of 0.001% to 10% at a constant frequency of 1 Hz for pure TPU and MREs containing 10–50 wt.% CIPs. Data are presented for both the off-state (0 A), where the magnetic particles are randomly distributed within the TPU matrix, and the on-state (4 A), where an external magnetic field of up to 0.624 T induces particle alignment and interparticle interactions. This dual-condition approach allows direct observation of both the inherent stiffness of the printed composites and their field-responsive behaviour.

In the off-state (0 A), where no external magnetic field was applied, all samples exhibited the characteristic strain-softening behaviour typical of viscoelastic elastomers. Within this regime, the storage modulus (G′) remained relatively constant at low strain amplitudes, corresponding to the LVE region, but decreased progressively as the applied shear strain increased. The reduction in G′ is attributed to the gradual breakdown of weak physical interactions within the elastomeric network, such as van der Waals forces and chain entanglements, as the material transitions from a predominantly elastic to a more viscous response. Incorporating CIPs had a clear and measurable effect on stiffness within the LVE region. Pure TPU exhibited the lowest baseline stiffness, with a G′ of 1.19 MPa, whereas the highest particle content sample, MRE50, achieved 1.67 MPa.

Table 4. Fabricated Pure TPU and MRE filaments diameter.

Sample	Diameter at a point (mm)										Average diameter (mm)
	1	2	3	4	5	6	7	8	9	10	
Pure TPU	1.74	1.75	1.74	1.74	1.73	1.74	1.75	1.71	1.75	1.73	**1.738**
MRE10	1.73	1.73	1.75	1.75	1.75	1.74	1.74	1.73	1.75	1.74	**1.741**
MRE20	1.75	1.73	1.74	1.75	1.74	1.70	1.75	1.75	1.74	1.75	**1.740**
MRE30	1.72	1.74	1.73	1.75	1.75	1.75	1.73	1.75	1.75	1.73	**1.740**
MRE40	1.74	1.72	1.75	1.74	1.75	1.72	1.74	1.74	1.74	1.75	**1.739**
MRE50	1.75	1.75	1.73	1.75	1.75	1.75	1.73	1.74	1.75	1.75	**1.745**

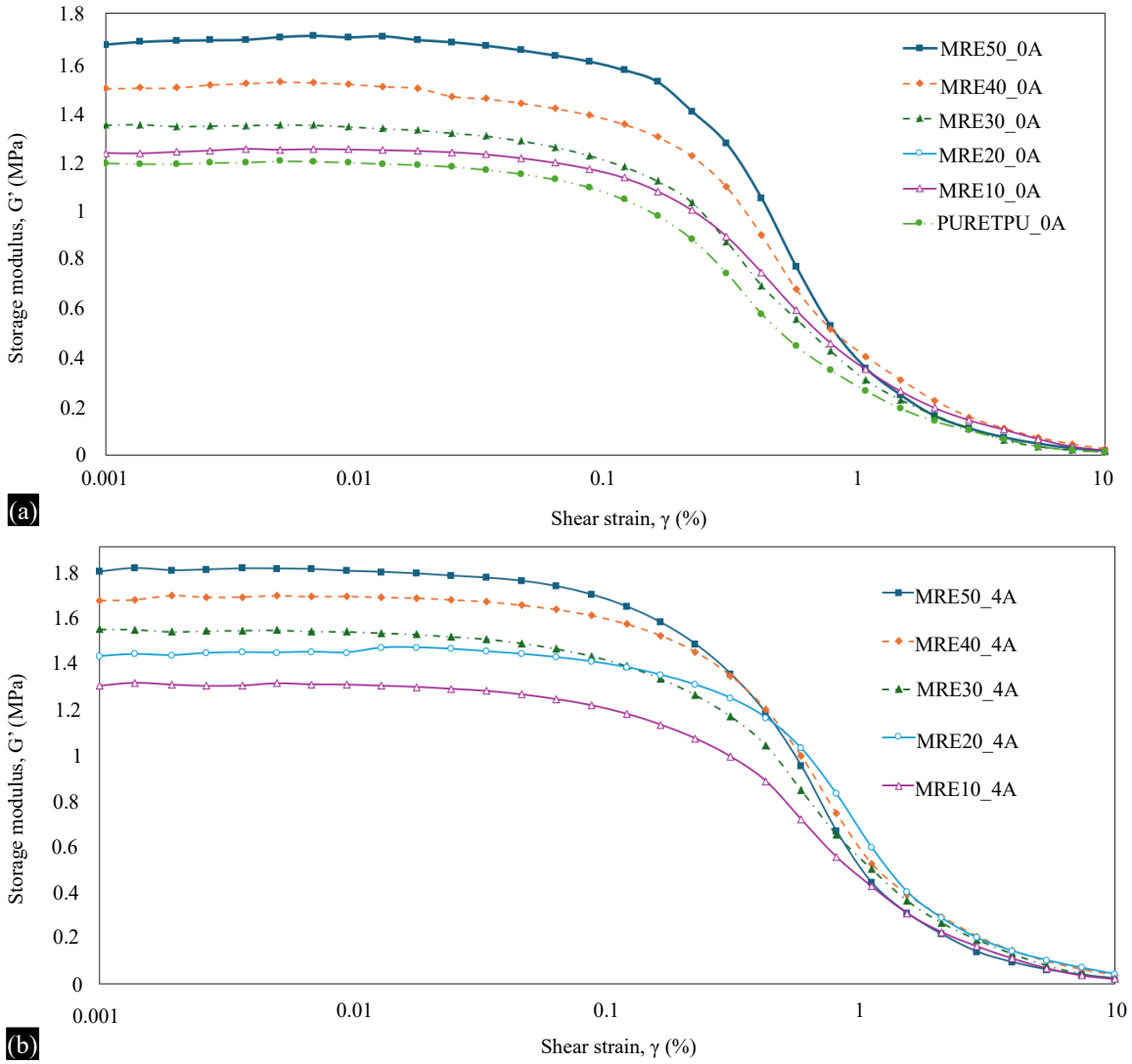

Figure 4. Storage modulus of printed MRE sample using FFF AM method on (a) off-state and (b) on-state conditions.

The upward trend in modulus with greater particle loading reflects the reinforcing role of rigid, micron-sized magnetic particles embedded in the soft TPU matrix.

The magnetic particles act as physical crosslink points that mechanically constrain surrounding polymer chains, limiting their ability to reorient under small strains. At higher loadings, reduced interparticle spacing further enhances this reinforcing effect by introducing additional resistance pathways to deformation and increasing the effective load-bearing capacity of the composite [14, 15]. Off-state stiffness improvement corresponds closely with the dimensional stability and hardness measurements presented in Section 3.1, where a similar upward trend in Shore A hardness was observed with increasing CIP content. The microstructural reinforcement imparted by the particles is therefore evident in both static (hardness) and dynamic (G′) mechanical tests. The relatively modest increase in modulus compared with mould-cast MREs is likely linked to directional particle alignment during filament extrusion in the FFF process, which can limit isotropic reinforcement throughout the bulk material.

Under the on-state condition (4 A), all MRE samples exhibited an increase in storage modulus (G′) compared to their corresponding off-state values, providing clear evidence of the magnetorheological

effect. The enhancement in stiffness is a direct consequence of field-induced particle alignment within the elastomeric matrix. When exposed to the magnetic field, CIPs tend to orient and form chain-like structures along the direction of the applied field. These newly formed particle chains create additional load-bearing pathways and reinforce the surrounding polymer matrix, thereby increasing resistance to shear deformation and shifting the material response towards a more elastic-dominated behaviour. The magnitude of the magnetorheological effect increased progressively with higher CIP concentrations, as a greater volume fraction of magnetic particles provides more potential for particle-particle interactions and chain formation under the influence of the magnetic field. However, the observed improvement in G′ was less pronounced than values reported for mould-cast or FGF-printed MREs [13]. For instance, FFF-printed MRE50 achieved a G′ of 1.80 MPa in the on-state, while an equivalent FGF-printed MRE50 from Sukarman et al. [13] reached 2.03 MPa under similar conditions. This discrepancy can be linked to the particle alignment characteristics inherent to the FFF process. During filament extrusion and subsequent layer-by-layer deposition, the shear forces and directional material flow promote preferential alignment of CIPs along the print path. Such anisotropic alignment enhances stiffness along certain orientations but reduces the isotropic connectivity needed for the formation of a dense, three-dimensional particle chain network when the field is applied. Consequently, the full potential of the magnetorheological effect is not realized in FFF-printed samples compared to those fabricated using methods that promote more uniform particle distribution, such as FGF or mould casting. Although quantitative switching times were not measured in this study, the oscillatory shear tests demonstrated immediate increases in storage modulus upon magnetic field application, confirming the rapid responsiveness of all MRE formulations regardless of CIP loading.

Figure 6 further illustrates the comparative performance by plotting both off-state and on-state storage modulus (G′) values of FFF-printed MREs against their FGF-printed counterparts. In the off-state, FFF samples consistently demonstrated higher baseline stiffness than those produced via FGF, with the most notable difference observed for pure TPU (1.19 MPa for FFF versus 0.91 MPa for FGF). This trend supports the conclusion that filament-based printing can produce stiffer base materials, likely due to the enhanced compaction and reduced void content achieved during the filament extrusion stage. The controlled filament diameter and precise feeding in FFF also contribute to denser, more uniform deposition, which in turn improves load-bearing capacity even without the presence of a magnetic field.

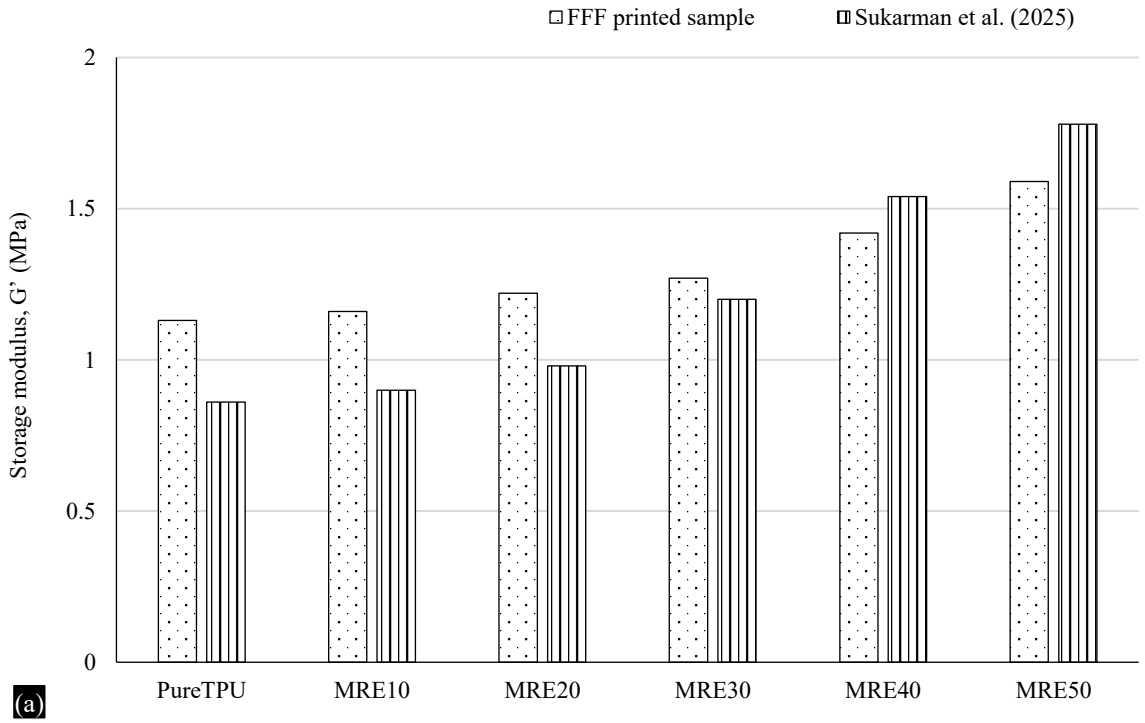

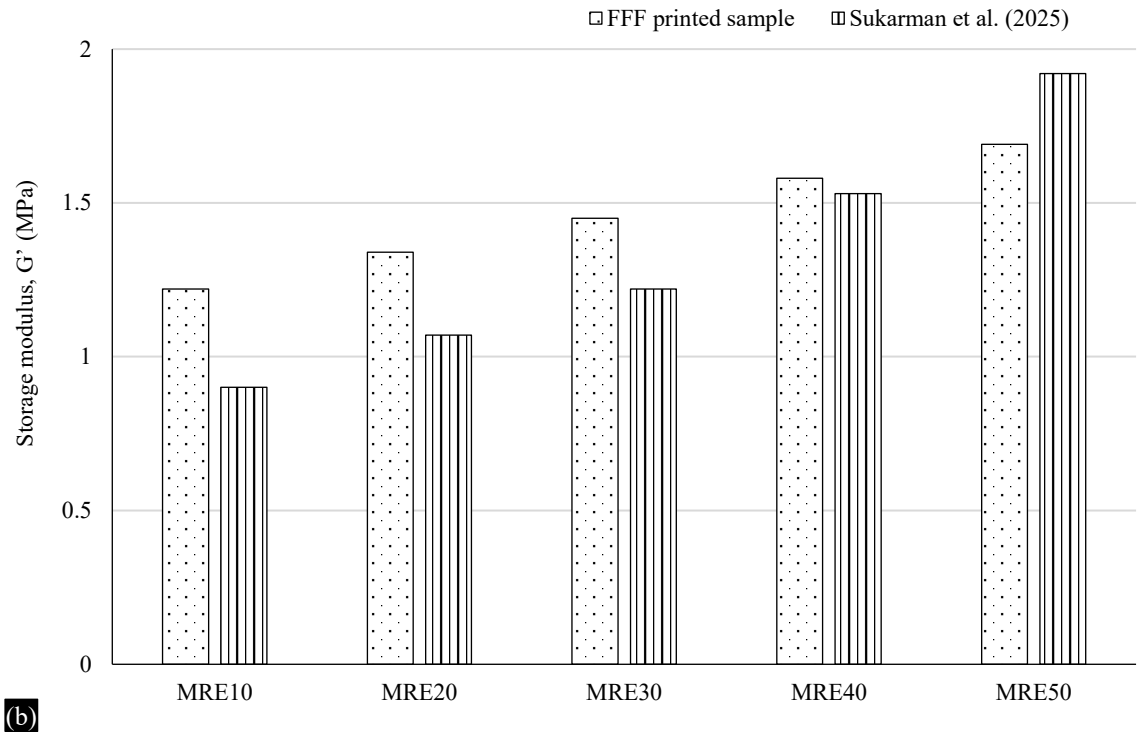

Figure 6. FFF-printed MRE samples against FGF-printed samples at (a) off-state and (b) on-state conditions.

In contrast, under the on-state, the magnetorheological effect was consistently lower for FFF samples across all CIP loadings. This reduced field responsiveness reflects a fundamental trade-off between achieving high baseline stiffness and maximizing the magneto-responsive performance. The layer-by-layer nature of FFF, combined with the shear forces present during filament extrusion, promotes preferential particle alignment along the print path. While this anisotropic arrangement benefits dimensional stability and stiffness along specific orientations, it can hinder the formation of a fully interconnected, isotropic three-dimensional particle chain network when the magnetic field is applied [16]. Such network formation is more readily achieved in FGF or mould-cast samples, where particle distribution is more random and uniform.

These findings directly reinforce the points established in the introduction, where FFF provides clear advantages in terms of dimensional accuracy, repeatability, and baseline stiffness, but its microstructural characteristics inherently limit the magnitude of the magnetorheological effect. This process–property relationship has significant implications for material selection in application-specific designs. For instance, FFF-printed MREs are likely to be more suitable for adaptive structural components, precision damping systems, or soft robotic actuators where geometric fidelity and inherent stiffness are critical design requirements. Conversely, FGF may remain the preferred fabrication route in applications, such as vibration isolation mounts or field-tunable devices, where maximizing the MR effect is of primary importance.

Compared with conventional moulding or casting, the 4D-printing approach via FFF demonstrated clear advantages in terms of dimensional precision, repeatability, and adaptability for complex geometries. While traditional methods are limited by tooling requirements, longer processing times, and lower design flexibility, the present work shows that FFF can achieve deviations below 5.5% even at 50 wt.% CIP concentration, with consistent magneto-responsiveness. These advantages highlight 4D printing as a more versatile and application-driven method, particularly in adaptive structures, tunable damping systems, and soft robotics.

CONCLUSION

This study successfully demonstrated the fabrication and preliminary characterization of 4D-printed MREs composed of TPU with varying CIP loadings, produced via the FFF method. All primary objectives were achieved in which the MRE filaments with controlled diameters were produced without defects, their printability and dimensional fidelity were confirmed, and their magneto-mechanical performance was evaluated through strain sweep rheological testing. The results showed that FFF-printed MREs consistently maintained high dimensional accuracy across all CIP concentrations and exhibited a progressive increase in stiffness with higher particle loading. However, while baseline stiffness in the off-state was higher than that of comparable FGF-printed samples, the magnetorheological effect in the on-state was comparatively lower, a difference attributed to the anisotropic particle alignment induced during filament extrusion and layer deposition in the FFF process. These findings provide clear insights into the trade-offs between precision, inherent stiffness, and field responsiveness in additively manufactured MREs. The results indicate that FFF offers significant advantages for producing high-precision components with stable baseline stiffness, making it suitable for applications, where dimensional accuracy and inherent rigidity are critical. Whereas FGF may remain the preferred fabrication method for applications that demand a higher magnetorheological effect.

Acknowledgements

This work was supported by Higher Institution Centre of Excellence (HiCOE) program of Ministry of Higher Education (MOHE) Malaysia under HiCOE Research Grant and the TVET Applied Research Grant Scheme (T-ARGS/2025/BK01/00578) under the Ministry of Finance (MOF) Malaysia.

Conflict of interest

The authors declare no conflict of interest.

REFERENCES

1. Gonzalez G, Roppolo I, Pirri CF, Chiappone A. Current and emerging trends in polymeric 3D printed microfluidic devices. Additive Manufacturing. 2022 Jul 1;55:102867.
2. Falahati M, Ahmadvand P, Safaee S, Chang YC, Lyu Z, Chen R, Li L, Lin Y. Smart polymers and nanocomposites for 3D and 4D printing. Materials today. 2020 Nov 1;40:215-45.
3. Rafiee M, Farahani RD, Therriault D. Multi-Material 3D and 4D Printing: A Survey. Advanced Science. 2020 Jun 30;7(12):1902307.
4. Bastola AK, Hossain M. A review on magneto-mechanical characterizations of magnetorheological elastomers. Compos B Eng. 2020 Nov 1; 200:108348.
5. Gupta C, Pallavi MB, Shet NK, Ghosh AK, Bandyopadhyay S, Mukhopadhyay P. Microstructure and mechanical performance examination of 3D printed acrylonitrile butadiene styrene thermoplastic parts. Polym Eng Sci. 2020 Nov 1;60(11):2770–81.
6. Moradi M, Lalegani Dezaki M, Kheyri E, Rasouli SA, Aghaee Attar M, Bodaghi M. Simultaneous FDM 4D printing and magnetizing of iron-filled polylactic acid polymers. J Magn Magn Mater. 2023 Feb 15; 568:170425.
7. Krueger H, Vaezi M, Yang S. 3D Printing of Magnetorheological Elastomers (MREs) Smart Materials. In: Proceedings of the 1st International Conference on Progress in Additive Manufacturing. Singapore: Research Publishing Services; 2014. p. 213–8.
8. Bastola AK, Hoang VT, Li L. A novel hybrid magnetorheological elastomer developed by 3D printing. Mater Des. 2017 Jan 15; 114:391–7.
9. Curmi A, Rochman A. Fused granulate fabrication of injection molding inserts from high-performance ULTEM 9085™ thermoplastic for cosmetic packaging industry. Progress in Additive Manufacturing. 2024 Oct 1;9(5):1381–92.
10. Kalle J, Joni K, Alexander S, Juhani O. Potential and Challenges of Fused Granular Fabrication in Patternmaking. International Journal of Metalcasting. 2023 Oct 1;17(4):2469–76.

11. Wang H, Lamichhane TN, Paranthaman MP. Review of additive manufacturing of permanent magnets for electrical machines: A prospective on wind turbine. Materials Today Physics. Elsevier Ltd; 2022; Vol.24: 100675.
12. Tasin MA, Aziz SAA, Mazlan SA, Johari MAF, Nordin NA, Yusuf SYM, et al. Magnetostriction Enhancement in Midrange Modulus Magnetorheological Elastomers for Sensor Applications. Micromachines (Basel). 2023 Mar 29;14(4):767.
13. Sukarman AF, Mohd Yusuf S, Mazlan SA, Nordin NA, Patel DM, Johari MAF, et al. 4D-printed TPU-based magnetorheological elastomer using simplified feedstock preparation. Polym Eng Sci. 2025 Apr 1;65(4):1977–87.
14. Wu C, Cheng C, El-Aty AA, Li T, Qin Y, Yang Q, et al. Influence of particles size and concentration of carbonyl iron powder on magnetorheological properties of silicone rubber-based magnetorheological elastomer. Mater Res Express. 2020 Aug 1; 7(8):086101.
15. Bastola AK, Paudel M, Li L. Dot-patterned hybrid magnetorheological elastomer developed by 3D printing. J Magn Magn Mater. 2020 Jan 15;494.
16. Muhazeli NS, Nordin NA, Mazlan SA, Rizuan N, Abdul Aziz SA, Abd Fatah AY, et al. Characterization of morphological and rheological properties of rigid magnetorheological foams via in situ fabrication method. J Mater Sci. 2019 Nov 15;54(21):13821–33.

